

High pressure adsorption, permeation and swelling of carbon membranes – measurements and modelling at up to 20 MPa

Nicolas Kruse^a, Yuliya Schießer^a, Norman Reger-Wagner^b, Hannes Richter^b, Ingolf Voigt^b, Gerd Braun^a, Jens-Uwe Repke^c

^aTH Köln, Betzdorfer Str. 2, 50679 Cologne, Germany

^bFraunhofer IKTS, Michael-Faraday-Str.1, 07629 Hermsdorf, Germany

^cTU Berlin, Straße des 17. Juni 135, 10623 Berlin, Germany

Abstract

A unique feature of inorganic membranes is the ability to operate at high temperature and pressure. Even supercritical solvents can be processed by these membranes, whereas polymer membranes tend to swell and consequently suffer from reduced selectivity and mechanical strength. Carbon membranes open new possibilities, e.g. the processing of high pressure, high temperature fluid streams directly in place or the use in membrane reactors for chemical reactions like H₂ synthesis by dehydrogenation. This work investigates high pressure adsorption of carbon membrane material for different gases at up to 12 MPa, the selectivity and permeance for CO₂/N₂ mixtures in a pressure range from 0.1 to 20 MPa and the swelling of carbon material exposed to Oxygen at up to 10 MPa. A model based on Maxwell-Stefan diffusion with parameters gained from measured adsorption and fluxes has been implemented to improve the understanding of the behaviour of high pressure separation with carbon membranes.

1. Introduction

Carbon membranes for gas separation are of scientific interest for more than three decades. Even in the early years some quite promising results were shown, e.g. by Koresh et al. [1]. The research up to now is mostly driven by the excellent selectivity and permeability performance of carbon membranes compared to other membrane types [2]. Nevertheless this performance advance was not sufficient yet to compete economically successfully with polymeric membranes.

However, for the separation of streams with harsh conditions, like high pressure and high temperature or supercritical media with high dissolving power, polymeric membranes suffer from reduced strength, caused by swelling and plasticization [3]. A high strength is mandatory because high pressure gas separation requires high transmembrane pressures as discussed in detailed by Huang et al. [4]. We assume that carbon membranes show a modest swelling as well because for other porous carbon materials this has been measured [5–7] before. That swelling might impact the gas transport, but carbon membranes do not notably deteriorate from reduced strength. Therefore they are very suitable candidates for high pressure membrane gas separation.

Despite this high potential, very limited research has been carried out on high pressure gas separation

with carbon membranes. This might have been caused by a lack of demand because established processes have been designed without considering the possible use of high pressure gas separation.

In recent years, a few journal articles have been published on gas separation with carbon membranes at pressures of 2 MPa and above. Only some of the published experiments are conducted with actual mixtures (Table 1 gives an overview of articles known to us).

Table 1
High pressure carbon membrane publications

Year	p_{max} / MPa	Experiment	Publication
1997	5.8	single gas	F.K. Katsaros et al. [8]
2002	7.0	mixture	D. Vu et al. [9]
2007	5.5	single gas	F.K. Katsaros et al. [10]
2007	2.6	single gas	K. Wang et al. [11]
2011	2.4	mixture	L. Xu et al. [12]
2012	3.0	mixture	R. Swaidan et al. [2]
2014	5.5	single gas	E. Favvas et al. [13]

2014	5.6	single gas	E. Favvas et al. [14]
2014	5.5	mixture	N. Bhuwania et al. [15]
2016	20.0	mixture	N. Kruse et al. [16]
2017	2.0	mixture	O. Salinas et al. [17]

The selective transport in carbon membranes is primarily characterised by size exclusion (molecular sieving) and adsorption phenomena. Koresh and Soffer [1] showed that the Fick's law can be applied by deriving the local concentrations from the adsorption isotherms of the components. For higher pressures this approach is not practical because the Fick diffusivity coefficients become strongly dependent on the local concentrations of all components.

The Maxwell–Stefan diffusion model overcomes this limitation by a different definition of the diffusion coefficients. Krishna [18,19] proposed for binary mixtures in zeolites and other crystalline materials the implementation shown in Eq. 1. Rungta et al. applied Maxwell–Stefan diffusion to carbon membranes as well [20,21].

$$-\frac{\rho q_1}{RT} \cdot \nabla \mu_1 = \frac{x_2 \cdot j_1 - x_1 \cdot j_2}{D_{12}} + \frac{j_1}{D_1} \quad \text{Eq. 1}$$

$$-\frac{\rho q_2}{RT} \cdot \nabla \mu_2 = \frac{x_1 \cdot j_2 - x_2 \cdot j_1}{D_{12}} + \frac{j_2}{D_2}$$

In Eq. 1 ρq is the volumetric adsorption, R the universal gas constant, T the temperature, μ the chemical potential, x the molar fraction in the adsorbate phase, j the molar flux, D_{12} the Maxwell–Stefan diffusion coefficient for gas to gas and D_1 and D_2 for gas to membrane interactions. Assuming no temperature gradients in the separation layer the chemical potential for each component can be described by the fugacity f_i :

$$d\mu_i = RT \frac{1}{f_i} df_i \quad \text{Eq. 2}$$

The adsorption equilibrium of the carbon material can be described by Langmuir isotherms for many gases at pressures up to 1 MPa [22]. However for higher pressures the Langmuir model, which is limited to mono layer adsorption, is no longer capable to approximate the measured adsorption behaviour for most gases. Eq. 3 describes the equilibrium loading q by the BET model proposed by Brunauer et al. [23]. This model overcomes the limitation by modelling multiple molecular layers. $q_{s,i}$ is the single layer saturation loading, b_i the sorption coefficient, $f_{s,i}$ the saturation fugacity and f_i the gas phase fugacity:

$$q_i = \frac{b_i q_{s,i} f_i}{(f_{s,i} - f_i) \cdot \left(1 + \frac{(b_i - 1)f_i}{f_{s,i}}\right)} \quad \text{Eq. 3}$$

The aim of this work is to contribute to a better understanding of the relevant mechanisms at high pressure mass transport in carbon membranes and thereby advancing membrane technology into new industrial applications.

2. Experimental

2.1 Samples

The tested membrane has a tubular configuration with an active surface of $5.3 \cdot 10^{-3} \text{ m}^2$. It has an inner diameter of 7 mm, outer diameter of 10 mm and a total length of 250 mm. The $2 \mu\text{m}$ thick carbon separation layer is coated on the inner side of a porous aluminium oxide support tube. Multiple intermediate layers ensure a smooth surface for the separation layer (Fig. 1). The membrane has been developed and manufactured by Fraunhofer IKTS/Hermsdorf. More details on the membrane were described previously [16].

The carbon bulk material for the adsorption and swelling experiments is fabricated in the same process as the membrane separation layer but without ceramic support and a thickness of approximately $100 \mu\text{m}$. For the bulk density of the material a value of 1.37 kg/dm^3 was determined. We assume that this sample material behaves quite similarly to the 50 times thinner separation layer. However, there might be effects in the preparation process that are not understood yet.

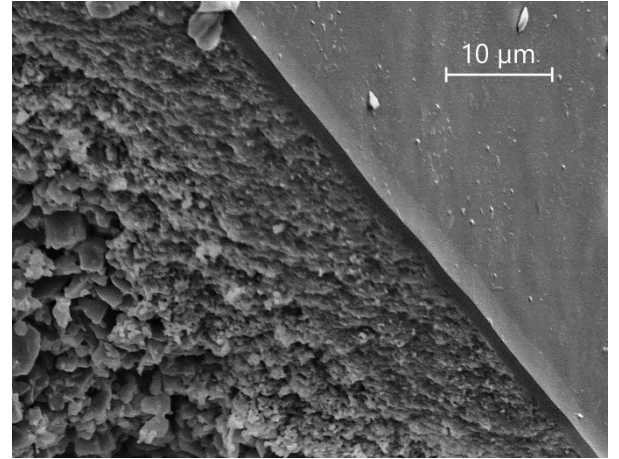


Fig. 1: SEM image shows the asymmetric structure of the carbon membrane

2.2 Measurements

In order to investigate the gas transport through the membrane, measurements with an equimolar mix-

ture composed of N₂ and CO₂ have been carried out at pressures up to 20 MPa. N₂ is supplied by a 30 MPa cylinder and CO₂ by a cooled high pressure pump. All measuring points were taken at steady state, at a retentate flow at least 20 times higher than the permeate flow to prevent any significant concentration gradients along the membrane tube. The feedback controlled mixing of the feed stream and analysis of the permeate stream composition is based on thermal conductivity sensors. The test plant and the construction of the membrane test cell has been described previously in detail [16].

The fugacities are determined by integrating equation of state data from Span et al. [24,25] with Kunz and Wagner mixing rules [26]. Separation factors S_{ij} are determined by the quotient of the measured molar component ratio on feed and permeate side as shown in Eq. 4.

$$S_{ij} = \frac{x_{i,p} / x_{j,p}}{x_{i,f} / x_{j,f}} \quad \text{Eq. 4}$$

The adsorption equilibrium of the membrane carbon material has been determined for the gases CO₂, N₂, CH₄ and O₂. Single gas adsorption measurements were measured gravimetrically with a Rubotherm magnetic suspension balance. To take competitive adsorption phenomena into account, binary mixtures of CO₂/N₂ were measured with a volumetric measuring apparatus as well. The analysis of the adsorbate gas phase was performed by NDIR and GC.

To study the swelling of the carbon membrane material at high pressure a test apparatus was developed as shown in Fig. 2.

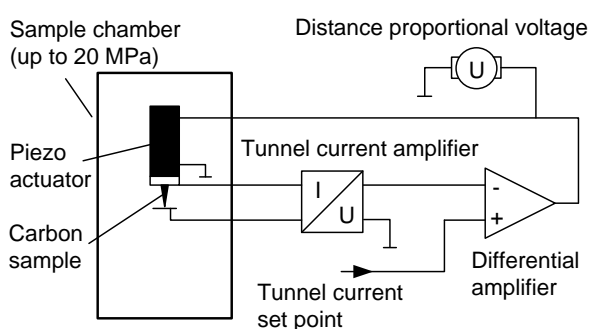


Fig. 2: Experimental setup for investigating high pressure swelling

The apparatus consists of a high pressure sample chamber with electrical feed-throughs as well as gas in- and outlets. Inside the chamber the sample is mounted on a preloaded piezo actuator supplied by PI Ceramic GmbH. The actuator can move the sample towards a gold plated electrode with an overall travel distance of

15 μm . Between the conductive carbon sample and the gold plated electrode a voltage of approximately 2 V is applied. The tunnel current between sample and the gold plated electrode is converted to a voltage by a transimpedance amplifier based on the low noise high precision operation amplifier OPA140AID from Texas Instruments. The amplifier is located directly at the high pressure sample chamber to keep the leads on the input side as short as possible. This prevents RF interferences and keeps the capacity low. The output voltage of the transimpedance amplifier is fed into an adjustable analog proportional-integral-controller. The controller uses a Texas Instruments OPA541AP high power operational amplifier to drive the piezo actuator with a Voltage of up to 50 V. This circuit controls the piezo driving voltage to maintain a constant tunnel current of about 1 nA. Therefore a constant distance between sample and electrode is maintained as well (below 1 nm). The resulting piezo driving voltage is therefore proportional to the elongation of the sample.

To compensate for the compressibility of the piezo material under pressure, an off-set reference measurement was carried out with a platinum wire in place of the carbon sample. Gross adjustments of the sample-electrode distance are done with a fine pitch setscrew coupled to a 10:1 reduction lever.

3. Results and discussion

3.1 Adsorption

The adsorption data connect the local fugacity inside the membrane to the local concentration. Therefore these data are essential to model the transport through the separation layer. Single gas adsorption measurements were carried out at a temperature of 298 K and pressures of up to 12 MPa. As expected the CO₂ adsorption at pressures below 0.1 MPa is significantly higher compared to the other investigated gases, whereas at elevated pressure the adsorption capacities converge. For N₂ the loading at low pressure is similar to O₂, which is shown in the literature as well [27], but for higher pressure the O₂ loading kept increasing whereas the slope of the Nitrogen loading flattens.

Only for N₂ the Langmuir model is capable to represent the measured data over the whole investigated pressure range. By applying the BET-model the adsorption of all investigated gases can be well described as shown in Fig. 3.

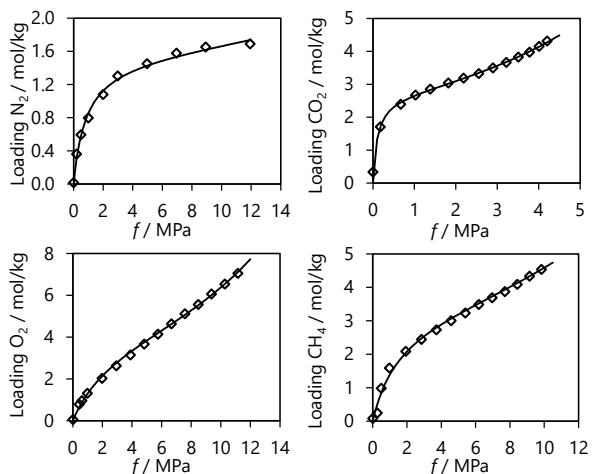


Fig. 3: Measured adsorption of the membrane material for different gases (\diamond) and the corresponding BET model fit (-)

Considering the microscopic scale it is to note that inside the selective pores of the carbon membrane multilayer adsorption, like proposed by the BET model, is hardly possible as the diameter of the selective pores is less than two molecule diameters [23]. This may indicate that the measured adsorption loading at high pressure is assigned to larger pores which are considered to be much less relevant for the transport properties of the membrane. The obtained sorption parameters are listed in Table 2.

Table 2
Sorption coefficient for the BET model

Gas	b_i	$f_{s,i}$ / MPa	$q_{s,i}$ / mol/kg
N ₂	87.2	73.4	1.54
CO ₂	105.1	10.6	2.61
O ₂	9.4	23.8	4.24
CH ₄	19.2	29.0	3.30

To model the adsorption of binary gas mixtures, equimolar CO₂/N₂ mixture were investigated as well. Because of the moderate deviation between this measurement and the single gas results (Fig. 4) the adsorption of the mixture components are assumed to be independent from each other. By applying the Ideal Adsorbed Solution Theory [28] the mixed gas adsorption can be approximated, but as Rother and Fieback pointed out even at a low pressure around 1 MPa the prediction accuracy is very low for carbon material [29].

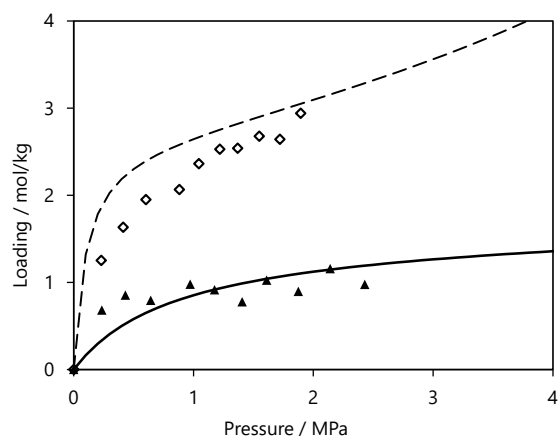


Fig. 4: Measured adsorption of the membrane material for an equimolar mixture of CO₂ (\diamond) and N₂ (\blacktriangle). The lines show the corresponding BET model fit for single gas measurements of CO₂ (- -) and N₂ (-).

3.2 Permeance

The measured multicomponent fluxes and adsorption data were used to obtain the coefficients of the Maxwell-Stefan diffusion model by multivariate regression. Table 3 shows the coefficients.

Table 3
Maxwell-Stefan diffusion coefficients

Symbol	$D \cdot 10^{-11}$ / m ² /s	Description
D_1	1.77	N ₂ / membrane
D_2	0.73	CO ₂ / membrane
D_{12}	0.52	N ₂ / CO ₂

For the regression start values for the three diffusion coefficients were roughly estimated and the system of differential equations Eq. 1 was numerically integrated over the separation layer thickness for each permeance experiment. The feed side fugacities, fluxes and adsorption equilibria were defined by the experimental data. The integration results give permeate side fugacity values which were compared to the measured values. Then, new diffusion coefficients were chosen and the integration step was repeated multiple times. By applying the Nelder–Mead method [30], the diffusion coefficients were systematically chosen in a way that the calculated permeate side fugacities converge with the measured fugacities.

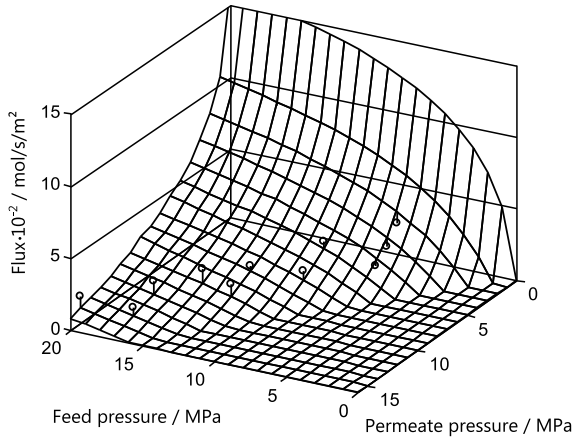


Fig. 5: Calculated flux for an equimolar N_2/CO_2 mixture at 298 K and measured data points (o) with vertical lines to show model deviations

Fig. 5 shows the flux calculated by the described model with the obtained parameters for an equimolar CO_2/N_2 mixture. As indicated in the diagram, only a fraction of the feed/permeate pressure combinations are covered by measured data. The measurements from this work are limited to a transmembrane pressure of 7 MPa due to the mechanical limitation of the membrane support. The calculated data for higher transmembrane pressure is therefore hypothetical, but can give a qualitative idea of which performance may be expected for a similar membrane under this condition.

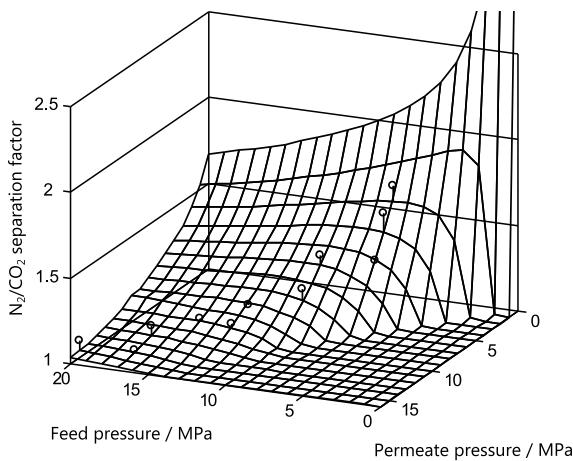


Fig. 6: Calculated separation factor for an equimolar N_2/CO_2 mixture at 298 K and measured data points (o) with vertical lines to show model deviations

For the calculated separation factors, the same limitations apply as well (Fig. 6). The shown peak for low pressure permeation is caused primarily by the significant higher adsorption of CO_2 at low pressure com-

pared to other investigated gases. At 10 kPa the measured single gas adsorption loading is approximately 30 times higher for CO_2 than N_2 . For higher pressures the ratio drops below 3. Due to the simplified implementation of mixed gas adsorption, this model may overestimate the adsorption selectivity and therefore the separation factor as well. But qualitatively this effect has been shown by other authors as well, e.g. by Swaidan et al. for CO_2/CH_4 [2].

The low sorption selectivity in the investigated pressure range is one reason for the low separation factors obtained by the permeance experiments. Furthermore the size and shape of N_2 and CO_2 molecules is very similar. Therefore a high sieving based selectivity is more difficult to achieve for this mixture compared to many others, but there is certainly still potential to tailor the membrane to this specific separation task.

The model assumes that the membrane separation layer is macroscopic isotropic and the support layer as well as the interface between separation layer and support layer is negligible for the mass transport. Solving the model provides an estimation of the local fugacity and adsorption loading of the components inside the separation layer. Fig. 7 shows exemplarily the results for an equimolar N_2/CO_2 mixture at 7 MPa feed pressure and 3 MPa permeate pressure.

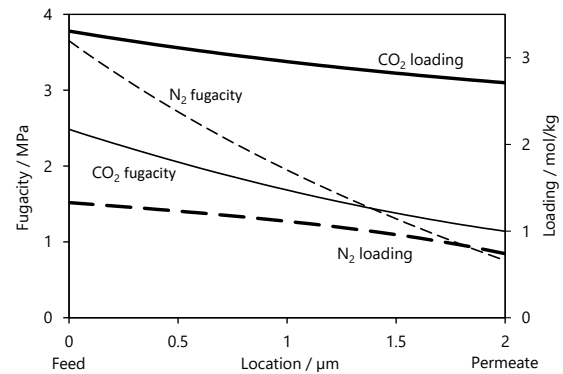


Fig. 7: Modelled fugacities and loadings inside the active layer on the path from feed to permeate side

This shows that the gradients are in some cases strongly location depended which has to be considered when modelling carbon membranes for high pressure gas transport.

3.3 Swelling

Swelling of the carbon membrane material was investigated with O_2 at a pressure of up to 10.5 MPa and a temperature of 294 K (Fig. 8). The adsorption measurements indicate that O_2 leads to a significant swelling, because it shows the highest maximum loading without

condensation (Fig. 3). Due to the high sample thickness of approximately 100 μm , it takes multiple hours to reach the equilibrium. The permeance experiments do not show this time dependent effect since the separation layer of the membrane is 50 times thinner. The down pointing spikes during the pressure change are caused by temperature changes from expanding O_2 into the sample chamber. This artefact is only temporally as the high thermal mass of the sample chamber equalizes this disturbance.

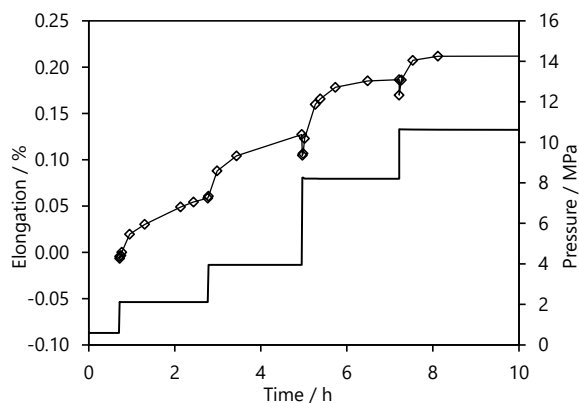


Fig. 8: Pressure (-) and time dependent elongation (\diamond) of the carbon membrane material in an O_2 atmosphere

The measured swelling effect (relative elongation per pressure) of up to 0.4 GPa^{-1} is small compared to reported values for activated carbon material of approximately 5 GPa^{-1} for CO_2 and 1.7 GPa^{-1} for CH_4 [5]. That is due to the less porous and therefore much more rigid structure of the membrane material compared to activated carbon. In both cases the swelling of the anisotropic graphene crystallites is partially inhibited by adjacent graphene layers with an orthogonal orientation. Due to the additional macro porosity of the activated carbon it is much more flexible and therefore the expansion is less inhibited.

Since the membrane pores are similar in size to the molecules, even very small size changes of the pores or the molecules result in a significant change in permeance. A size difference of 0.05 nm can result at least in an permeance change of an order of magnitude [21,31,32]. The measured elongation ε of 0.2 % (Fig. 2) can be assigned to a change of pore volume, whereas the volume of the carbon skeleton is fixed. That means that the macroscopic elongation of the sample and the microscopic relative pore size change can be linked by the fraction of accessible pore volume (Eq. 5). The pore size d_p is assumed to be roughly 0.5 nm and the upper bound of the pore volume fraction ϕ is given by the ratio of the measured bulk density ρ_b and the density of ideal graphite ρ_g .

$$\varepsilon = \frac{\Delta d_p}{d_p} \phi = \frac{\Delta d_p \rho_b}{d_p \rho_g} \quad \text{Eq. 5}$$

The actual pore size change is higher than estimated by this calculation, but the result gives a lower limit for the size change Δd_p of 0.0016 nm. This change has certainly no major impact for the transport, but it might be still large enough for being not fully negligible and affects the permeance in the range of a few percent.

4. Conclusion

High pressure adsorption, permeance and swelling experiments have been carried out to investigate the behaviour of carbon membranes for high pressure separation at up to 20 MPa. The adsorption data clearly show that at high pressure condition the Langmuir behaviour does not apply for most gases, whereas the BET model fits the data very well. If this behaviour is caused by multilayer adsorption in large, non-selective pores of the carbon membrane material or other phenomena is still up to further research.

A model based on Maxwell-Stefan diffusion has been applied to study the membrane behaviour at high pressure conditions. The model gives an overview of the expected carbon membrane performance over a large range of feed and permeate side pressures. The results make clear, that for an operation at high pressure on the permeate side, a sufficient transmembrane pressure is mandatory to keep a substantial difference of fugacity for the better permeating component between feed and permeate side. Otherwise, the separation factor is limited by the lack of driving potential.

An apparatus was developed, which is capable to measure the swelling of the membrane material under high pressure. The measurement shows clearly an expansion of the membrane material proportional to the applied pressure. Therefore the expansion effect is only at high pressure significant for the mass transport through the membrane and even at high pressure the impact may be quite modest. To link the membrane expansion to the mass transport further research is required. The challenge here is to separate the effect of the swelling and the effect of the gas presence itself.

5. References

- [1] J.E. Koresh, A. Soffer, Mechanism of permeation through molecular-sieve carbon membrane. Part 1. — The effect of adsorption and the dependence on pressure, J. Chem. Soc. Faraday Trans. 1 Phys. Chem. Condens. Phases. 82 (1986) 2057. doi:10.1039/f19868202057.
- [2] R. Swaidan, X. Ma, E. Litwiller, I. Pinnau, High

- pressure pure- and mixed-gas separation of CO₂/CH₄ by thermally-rearranged and carbon molecular sieve membranes derived from a polyimide of intrinsic microporosity, *J. Memb. Sci.* 447 (2013) 387–394. doi:10.1016/j.memsci.2013.07.057.
- [3] W. Ogieglo, L. Upadhyaya, M. Wessling, A. Nijmeijer, N.E. Benes, Effects of time, temperature, and pressure in the vicinity of the glass transition of a swollen polymer, *J. Memb. Sci.* 464 (2014) 80–85. doi:10.1016/j.memsci.2014.04.013.
- [4] Y. Huang, T.C. Merkel, R.W. Baker, Pressure ratio and its impact on membrane gas separation processes, *J. Memb. Sci.* 463 (2014) 33–40. doi:10.1016/j.memsci.2014.03.016.
- [5] L. Perrier, F. Plantier, D. Grégoire, A novel experimental setup for simultaneous adsorption and induced deformation measurements in microporous materials, *Rev. Sci. Instrum.* 88 (2017) 35104. doi:10.1063/1.4977595.
- [6] N. Kobayashi, T. Enoki, C. Ishii, K. Kaneko, M. Endo, Gas adsorption effects on structural and electrical properties of activated carbon fibers, *J. Chem. Phys.* 109 (1998) 1983. doi:10.1063/1.476774.
- [7] J.E. Koresh, On the flexibility of the carbon skeleton, *J. Chem. Soc. Faraday Trans.* 89 (1993) 935. doi:10.1039/ft9938900935.
- [8] F.K. Katsaros, T. a. Steriotis, A.K. Stubos, A. Mitropoulos, N.K. Kanellopoulos, S. Tennison, High pressure gas permeability of microporous carbon membranes, *Microporous Mater.* 8 (1997) 171–176. doi:10.1016/S0927-6513(96)00080-6.
- [9] D.Q. Vu, W.J. Koros, S.J. Miller, High Pressure CO₂/CH₄ Separation Using Carbon Molecular Sieve Hollow Fiber Membranes, *Ind. Eng. Chem. Res.* 41 (2002) 367–380. doi:10.1021/ie010119w.
- [10] F.K. Katsaros, T.A. Steriotis, G.E. Romanos, M. Konstantakou, A.K. Stubos, N.K. Kanellopoulos, Preparation and characterisation of gas selective microporous carbon membranes, *Microporous Mesoporous Mater.* 99 (2007) 181–189. doi:10.1016/j.micromeso.2006.07.041.
- [11] K. Wang, L.S. Loo, K. Haraya, CO₂ Permeation in Carbon Membranes with Different Degrees of Carbonization, *Ind. Eng. Chem. Res.* 46 (2007) 1402–1407. doi:10.1021/ie060617a.
- [12] L. Xu, M. Rungta, W.J. Koros, Matrimid® derived carbon molecular sieve hollow fiber membranes for ethylene/ethane separation, *J. Memb. Sci.* 380 (2011) 138–147. doi:10.1016/j.memsci.2011.06.037.
- [13] E.P. Favvas, Carbon dioxide permeation study through carbon hollow fiber membranes at pressures up to 55bar, *Sep. Purif. Technol.* 134 (2014) 158–162. doi:10.1016/j.seppur.2014.07.041.
- [14] E.P. Favvas, A.C. Mitropoulos, N.K. Kanellopoulos, CO₂ Permeability through Carbon Hollow Fiber Membranes from Atmospheric Pressure Up to 56 bar, in: *Int. Conf. Biol. Civ. Environ. Eng. March 17-18, 2014 Dubai, International Institute of Chemical, Biological & Environmental Engineering, 2014.* doi:10.15242/IICBE.C0314115.
- [15] N. Bhuvania, Y. Labreche, C.S.K. Achoundong, J. Baltazar, S.K. Burgess, S. Karwa, et al., Engineering substructure morphology of asymmetric carbon molecular sieve hollow fiber membranes, *Carbon N. Y.* 76 (2014) 417–434. doi:10.1016/j.carbon.2014.05.008.
- [16] N. Kruse, Y. Schießler, S. Kämnitz, H. Richter, I. Voigt, G. Braun, et al., Carbon membrane gas separation of binary CO₂ mixtures at high pressure, *Sep. Purif. Technol.* 164 (2016) 132–137. doi:10.1016/j.seppur.2016.03.035.
- [17] O. Salinas, X. Ma, Y. Wang, Y. Han, I. Pinnau, Carbon molecular sieve membrane from a microporous spirobisindane-based polyimide precursor with enhanced ethylene/ethane mixed-gas selectivity, *RSC Adv.* 7 (2017) 3265–3272. doi:10.1039/C6RA24699K.
- [18] R. Krishna, The Maxwell–Stefan description of mixture diffusion in nanoporous crystalline materials, *Microporous Mesoporous Mater.* 185 (2014) 30–50. doi:10.1016/j.micromeso.2013.10.026.
- [19] R. Krishna, Describing the diffusion of guest molecules inside porous structures, *J. Phys. Chem. C.* 113 (2009) 19756–19781. doi:10.1021/jp906879d.
- [20] M. Rungta, G.B. Wenz, C. Zhang, L. Xu, W. Qiu, J.S. Adams, et al., Carbon molecular sieve structure development and membrane performance relationships, *Carbon N. Y.* 115 (2017). doi:http://dx.doi.org/10.1016/j.carbon.2017.01.015.
- [21] M. Rungta, L. Xu, W.J. Koros, Structure-performance characterization for carbon molecular sieve membranes using molecular scale gas probes, *Carbon N. Y.* 85 (2015) 429–442. doi:10.1016/j.carbon.2015.01.008.
- [22] M.C. Campo, F.D. Magalhães, A. Mendes, Comparative study between a CMS membrane and a CMS adsorbent: Part I-Morphology, adsorption equilibrium and kinetics, *J. Memb. Sci.* 346 (2010) 15–25.

- doi:10.1016/j.memsci.2009.08.045.
- [23] S. Brunauer, P.H. Emmett, E. Teller, Adsorption of Gases in Multimolecular Layers, *J. Am. Chem. Soc.* 60 (1938) 309–319. doi:10.1021/ja01269a023.
- [24] R. Span, W. Wagner, A New Equation of State for Carbon Dioxide Covering the Fluid Region from the Triple-Point Temperature to 1100 K at Pressures up to 800 MPa, *J. Phys. Chem. Ref. Data.* 25 (1996) 1509. doi:10.1063/1.555991.
- [25] R. Span, E.W. Lemmon, R.T. Jacobsen, W. Wagner, A. Yokozeki, A Reference Equation of State for the Thermodynamic Properties of Nitrogen for Temperatures from 63.151 to 1000 K and Pressures to 2200 MPa, *J. Phys. Chem. Ref. Data.* 29 (2000) 1361–1433. doi:10.1063/1.1349047.
- [26] O. Kunz, R. Klimeck, W. Wagner, M. Jaeschke, The GERG-2004 Wide-Range Equation of State for Natural Gases and Other Mixtures, 2007. doi:10.1021/je300655b.
- [27] W.N.W. Salleh, A.F. Ismail, Effects of carbonization heating rate on CO₂ separation of derived carbon membranes, *Sep. Purif. Technol.* 88 (2012) 174–183. doi:10.1016/j.seppur.2011.12.019.
- [28] A.L. Myers, J.M. Prausnitz, Thermodynamics of mixed-gas adsorption, *AIChE J.* 11 (1965) 121–127. doi:10.1002/aic.690110125.
- [29] J. Rother, T. Fieback, Multicomponent adsorption measurements on activated carbon, zeolite molecular sieve and metal–organic framework, *Adsorption.* 19 (2013) 1065–1074. doi:10.1007/s10450-013-9527-2.
- [30] J. a. Nelder, R. Mead, A simplex method for function minimization, *Comput. J.* 7 (1964) 308–313. doi:10.1093/comjnl/7.4.308.
- [31] H. Richter, H. Voss, N. Kaltenborn, S. Kämnitz, A. Wollbrink, A. Feldhoff, et al., High-Flux Carbon Molecular Sieve Membranes for Gas Separation, *Angew. Chemie Int. Ed.* (2017) 1–5. doi:10.1002/anie.201701851.
- [32] K. Briceño, A. Iulianelli, D. Montané, R. Garcia-Valls, A. Basile, Carbon molecular sieve membranes supported on non-modified ceramic tubes for hydrogen separation in membrane reactors, *Int. J. Hydrogen Energy.* 37 (2012) 13536–13544. doi:10.1016/j.ijhydene.2012.06.069.